Heliyon

ELSEVIER

Received:
8 April 2017
Revised:
17 July 2017
Accepted:
2 August 2017

Cite as:
Emmanuel I. Unuabonah, Adewale Adewuyi, Matthew O. Kolawole, Martins O. Omorogie, Olalekan C. Olatunde, Scott O. Fayemi, Christina Günter, Chukwunonso P. Okoli, Foluso O. Agunbiade, Andreas Taubert. Disinfection of water with new chitosan-modified hybrid clay composite adsorbent. Heliyon 3 (2017) e00379.
doi: 10.1016/j.heliyon.2017.e00379

Disinfection of water with new chitosan-modified hybrid clay composite adsorbent

Emmanuel I. Unuabonah [a,*], Adewale Adewuyi [a], Matthew O. Kolawole [b], Martins O. Omorogie [a], Olalekan C. Olatunde [a], Scott O. Fayemi [c], Christina Günter [d], Chukwunonso P. Okoli [c,f], Foluso O. Agunbiade [a,g], Andreas Taubert [h]

[a] *Environmental & Chemical Processes Research Laboratory, Department of Chemical Sciences, Redeemer's University, P.M.B 230, Ede, Osun State, Nigeria*

[b] *Department of Microbiology, University of Ilorin, Ilorin, Kwara State, Nigeria*

[c] *Department of Biological Sciences, Redeemer's University, P.M.B 230, Ede, Osun State, Nigeria*

[d] *Department of Earth and Environmental Science, University of Potsdam, D-14476 Potsdam, Germany*

[e] *Adsorption & Catalysis Research Laboratory, Department of Chemistry, Vaal University of Technology, Private Bag X021, Andries Potgieter Boulevard, Vanderbijlpark, 1900, South Africa*

[f] *Analytical/Environmental Chemistry Unit, Department of Chemistry/Biochemistry, Federal University Ndufu-Alike Ikwo, Ebonyi State, Nigeria*

[g] *Department of Chemistry, Faculty of Science, University of Lagos, Akoka, Lagos, Nigeria*

[h] *Institute of Chemistry, University of Potsdam, D-14476 Potsdam, Germany*

* Corresponding author.

E-mail addresses: unuabonahe@run.edu.ng, iyaemma@yahoo.com (E.I. Unuabonah).

Abstract

Hybrid clay composites were prepared from Kaolinite clay and *Carica papaya* seeds via modification with chitosan, Alum, NaOH, and $ZnCl_2$ in different ratios, using solvothermal and surface modification techniques. Several composite adsorbents were prepared, and the most efficient of them for the removal of gram negative enteric bacteria was the hybrid clay composite that was surface-modified with chitosan, Ch-nHYCA$_{\mathbf{1:5}}$ (Chitosan: nHYCA = 1:5). This composite adsorbent had a maximum adsorption removal value of 4.07×10^6 cfu/mL for *V. cholerae* after 120 min, 1.95×10^6 cfu/mL for *E. coli* after ~180 min and 3.25×10^6 cfu/mL for *S. typhi* after 270 min. The Brouers-Sotolongo model was found to better predict the maximum adsorption capacity (q_{max}) of Ch-nHYCA$_{1:5}$ composite adsorbent for the removal of *E. coli* with a q_{max} of 103.07 mg/g (7.93×10^7 cfu/

http://dx.doi.org/10.1016/j.heliyon.2017.e00379

mL) and *V. cholerae* with a q_{max} of 154.18 mg/g (1.19×10^8 cfu/mL) while the Sips model best described *S. typhi* adsorption by Ch-nHYCA$_{\mathbf{1:5}}$ composite with an estimated q_{max} of 83.65 mg/g (6.43×10^7 cfu/mL). These efficiencies do far exceed the alert/action levels of ca. 500 cfu/mL in drinking water for these bacteria. The simplicity of the composite preparation process and the availability of raw materials used for its preparation underscore the potential of this low-cost chitosan-modified composite adsorbent (Ch-nHYCA$_{\mathbf{1:5}}$) for water treatment.

Keywords: Environmental science, Physical chemistry, Materials science

1. Introduction

Disinfection of microbially contaminated water is a crucial step in water purification because the presence of waterborne pathogenic microbes has been linked to various diseases in humans. The presence of these bacteria in surface and ground water has rendered water in some parts of the world unsafe for drinking purposes, as they are the leading causes of several illnesses [1, 2]. Microbial contaminants have been identified to include human pathogens and free-living microbes [3, 4] with their primary sources being through domestic activities and agricultural processes [2]. In essence, there is a high likelihood of most water sources being contaminated by these microbial entities. The public health implication of microbial water pollution is, therefore, attracting wide attention.

It is reported that on an annual basis, millions of children worldwide die as a consequence of ingesting harmful pathogens in drinking water. Developing and developed countries of the world continue to face the problem of microbial contamination of water with Africa and Asia being the worst hit when compared to Europe [5]. Cholerae (*Vibro)*, typhoid fever (*Salmonella*) and dysentery (*Shigella*) are the major water-borne diseases in the developing countries. Meanwhile, acute gastroenteritis (enteric viruses), Cryptosporidiosis (*Cryptosporidium)*, and legionellosis (*Legionella)* are the major water-borne problems in Europe and US, and these arise majorly due to water distribution problems [6, 7].

Several treatment options have been considered and applied in the disinfection of water polluted with harmful pathogens; some of these treatments include; chemical disinfection, magnetic field, membrane filtration and adsorption [8, 9, 10]. Apart from the fact that chemical treatment with chlorine results in harmful and carcinogenic disinfection by-products [11], it is now implicated in the formation of chlorine-induced antibiotic resistance exhibited by bacteria [12, 13]. Membrane filtration, though very useful for disinfection of water, suffers from fouling which results in frequent replacement of the membranes that raises the cost of the entire treatment process. Recently, adsorption technique has been a favoured method to remove bacteria and viruses in water due to its simplicity, high efficiency, relatively cheap, easily regenerated and readily available [14]. Furthermore,

http://dx.doi.org/10.1016/j.heliyon.2017.e00379

adsorption process does not produce toxic disinfection by-products unlike in chemical disinfection methods.

From the preceding, there is an obvious need for increased attention aimed at getting rid of these microbes in drinking water to make the water safe for drinking. Several adsorbents have been evaluated for adsorption, some of which include both conventional and non-conventional materials [15] but over time nanoparticles have found wide acceptance for the removal of bacteria from water [16, 17, 18]. However, there are now growing concerns about their toxicity both to man and the environment, especially with silver-mediated nanoparticles [16, 19, 20]. This has led to a growing need for materials with excellent treatment capacities, which are non-toxic, cheap and readily available. Our previous studies using *Carica papaya* seeds for the removal of contaminants from water shows how efficient these seeds are [21, 22]. However, they degrade in water with time and thus produce treated water with a foul smell. To circumvent this, we developed a composite from both Kaolinite clay and *Carica papaya* seeds which proved to be an adsorbent with high adsorption capacity for removing inorganic and organic pollutants from water [23, 24], the composite being environmentally friendly with an upscaling potential. However, this material lacked the ability to remove bacteria from water (unpublished study).

In response to the growing need for low-cost but efficient materials for removal of bacteria from water and in an effort to build on our previous work, this study report the successful preparation of a new class of composite adsorbents from a mixture of Kaolinite clay, chitosan, $ZnCl_2$, Alum [$KAl(SO_4)_2.12H_2O$] and *Carica papaya* seeds via oven and microwave assisted conditions. Both Zn and Chitosan have antibacterial properties. The introduction of Zn into the composites is to improve the disinfection property of the composites since Zn is biocidal. Even though Zn is biocidal yet it is found in cells throughout the body. It is needed for the body's defensive (immune) system to properly work. It plays several other roles in the human body which include cell division, cell growth, wound healing, and the breakdown of carbohydrates. Zinc is also needed for the senses of smell and taste. It was used in preparing the materials utilised in this study, and it is not in any way harmful to human health in the event that it leaches into solution. An initial study of the analysis of Zn in water treated with Zn modified hybrid clay material suggests that the amount of Zn leached into treated water is far below WHO standard limit for Zn in drinking water [25]. Alum, on the other hand, has been used as a flocculant in water treatment but is used as a cheap source of Aluminium (Al) in this study in order to study the influence of Al in the composite on the removal of harmful pathogens from water. The composite adsorbents prepared in this study were used to rapidly remove enteric bacteria (*E. coli, S. typhi and V. cholerae*) from contaminated water. The raw materials for the preparation of these

http://dx.doi.org/10.1016/j.heliyon.2017.e00379

composite adsorbents are readily available and cheap to obtain. The entire disinfection process is straightforward and sustainable.

2. Materials and methods

2.1. Materials

Kaolinite clay was obtained from the Redemption Camp, Mowe, Ogun State, Nigeria. The clay mineral was purified according to a method described by Adebowale et al. [26]. *Carica papaya* seeds and commercial Alum [$KAl(SO_4)_2.12H_2O$] were obtained from the open market in Nigeria. Low molecular weight Chitosan (Sigma-Aldrich) with 77% deacetylation and $ZnCl_2$ (Sigma-Aldrich) were supplied by Bristol Scientific Company, Nigeria. The test microorganisms *Escherichia coli* (ATCC 25922), *Vibro cholerae* (ATCC 25837), and *Salmonella typhimurium* (ATCC 13311) were obtained from the Biological Sciences Department, Redeemer's University, Ede, Nigeria.

2.2. Synthesis of hybrid clay composite

2.2.1. Hybrid clay preparation

Hybrid clay composite material was prepared via the synthesis route described by Unuabonah, et al. [23]. Equal weights of Kaolinite clay and papaya seeds were soaked in 0.1 M of NaOH with occasional stirring for three days. The mixture was oven dried at 105 °C and calcined in a furnace at 300 °C for 6 h. The calcined material was washed with distilled water until neutral pH and was subsequently sieved to an average size of 50 μm. This composite material was labelled as *nHYCA*.

2.2.2. Modified hybrid clay composites

Chitosan modified hybrid clay composite was prepared using the method described by Silver, et al. [50]. Chitosan powder (1 g) was dissolved in 5% CH_3COOH with heating and stirring at 45 °C for 2 h. The chitosan solution was then slowly added to a suspension of either 3 g or 5 g nHYCA material with stirring. The mixture was stirred for 24 h at 55 °C. The thick slurry formed was allowed to cool to room temperature. A 1 M NaOH solution was subsequently used to precipitate the chitosan-nHYCA (Ch-nHYCA) composite adsorbent from solution. The precipitate was filtered and washed with 0.01 M HCl solution and distilled water to a neutral pH. The Ch-nHYCA composite adsorbent was dried in an oven at 60 ^oC, and after which it was crushed with a mortar and pestle to fine particles and kept for further use. The composite prepared with 2 g and 5 g nHYCA were labelled as Ch-nHYCA$_{\mathbf{1:2}}$ and Ch-nHYCA$_{\mathbf{1:5}}$ composite adsorbents respectively.

http://dx.doi.org/10.1016/j.heliyon.2017.e00379

Alum modified hybrid clay composite (Al-zHYCA) was prepared by forming a slurry from different weights of Kaolinite clay, *Carica papaya* seeds, $ZnCl_2$, NaOH, and commercial alum in the ratio 1:1:1:1:1 and 1:1:1:1:2 wt/wt respectively using distilled-deionized water. The slurry was transferred into a porcelain crucible and heated in a microwave oven at 540 Hz for 15 min. The composite adsorbent was left to cool to room temperature and washed with distilled-deionized water to neutral pH. The samples were dried in an oven at 105 °C and were subsequently labelled as Al-zHYCA$_{\mathbf{1:1}}$ and Al-zHYCA$_{\mathbf{2:1}}$ composite adsorbents based on the ratio of Alum to other components in the composites.

However, for Chitosan-zinc modified HYCA, zinc-modified hybrid clay (zHYCA) was first prepared by forming a slurry from equal weights of Kaolinite clay, *Carica papaya* seeds and $ZnCl_2$ which was then transferred into a porcelain crucible and heated in a microwave oven at 540 Hz for 15 min. The material produced (zHYCA) was washed several times with distilled-deionized water until a clear solution was obtained and then transferred into an oven to dry at 105 °C. The dried product was surface-modified with Chitosan in ratios of 1:1 and 1:2 wt/wt (chitosan: zHYCA) in a similar manner as that for Ch-nHYCA composite adsorbents earlier described.

2.3. Characterization

The composite adsorbents prepared were characterised using different characterization techniques. The morphology and elemental composition of the prepared composites were analysed using a JEOL JSM 6510 Scanning electron microscope equipped with an Oxford EDX spectrometer.

X-ray diffraction (XRD) patterns were recorded from 3.0 to 70° 2θ on a Siemens D-5000 diffractometer at 0.02° S^{-1}. The Fourier transformed infrared spectroscopy spectra of the composites were recorded using a Shimadzu FT-IR 8400S machine.

The point of zero charges (pH_{pzc}) of the composites, which is the pH at which the difference between the initial and final pH (ΔpH) is zero, was determined by the salt addition method described by Unuabonah et al. [23].

2.4. Antibacterial activity studies

Adsorption capacities of the prepared composite adsorbents for removal of test enteric bacteria (*E. coli, S. typhi* and *V. cholerae*) were determined by batch adsorption technique.

To obtain the concentration for the three test enteric bacteria: *E. coli, S. typhi,* and *V.* cholera, an initial efficiency test was carried out using a modified method described by Karunakaran & Vinayagamoorthy, [27]. Nutrient broth cultures were prepared by dissolving 13 g of nutrient broth in 1 L of distilled water, followed by

http://dx.doi.org/10.1016/j.heliyon.2017.e00379

sterilisation in an autoclave at 121 °C. The bacteria were inoculated into nutrient broths from a 'bijou' bottle and incubated for 24 h at 37 °C. The bacteria cells were measured using a Shidmazu UV 1650 pc spectrophotometer at 600 nm. The cells were harvested by centrifugation at 3000 rpm for 15 min and washed twice with sterile distilled water. The obtained bacterial cells were dispersed in sterile distilled water and the amount of colony forming units/mL (cfu/mL) obtained was determined by optical density technique with all three test bacteria given a concentration of ca. 1×10^8 cfu/mL using Eq. (1) for the calculation. This concentration was used for the initial efficiency test for the composite adsorbents prepared in which 30 mg of the composite adsorbent was added to 10 ml of 1×10^8 cfu/mL bacteria concentration at a pH of 7.08 and agitated for 6 h. The mixture was allowed to settle via sedimentation, and the supernatant solution was evaluated for the presence of bacteria using the optical density method that utilises a UV spectrophotometer at 600 nm. The process was repeated twice, and the percentage residue of the bacteria was determined from the average optical density readings. The result from this step was used to determine the most efficient adsorbent that was subsequently used for adsorption studies.

1.0 Absorbance = 1×10^8 cfu/ml [28] (1)

2.5. Adsorption equilibrium studies

Adsorption equilibrium studies were done by carrying out serial dilutions with the stock concentration of 1×10^8 cfu/mL for each bacterium, in other to prepare the various concentrations of bacteria in the range of 35 mg/L to 1000 mg/L using Eq. (2).

Absorbance = 0.39 g/L dry weight of bacteria cells [29] (2)

The batch adsorption technique was used. Based on the results from initial efficiency test, 30 mg of Ch-nHYCA$_{\mathbf{1:5}}$ composite adsorbent (being the most efficient test composite adsorbent) was used for further experiments to remove the bacteria from 10 ml solution of a known concentration of the bacteria in aqueous solutions at room temperature and at a pH of ca. 7.1. The mixture was agitated for 6 h in a rotatory shaker and then allowed to sediment. The concentration of bacteria in the supernatant test solution at equilibrium was then measured using the optical density method at 600 nm in a UV 1650 pc spectrophotometer (Shimadzu). The amount of bacteria adsorbed by the adsorbent (q_e) was calculated using Eq. (3).

$$q_e = \frac{(C_o - C_e) \times V}{w} \quad (3)$$

Where q_e (mg bacteria/g adsorbent) is the adsorbed amount of bacteria held on the composite adsorbent, C_o (mg bacteria/L solution) and C_e (mg bacteria/L solution)

http://dx.doi.org/10.1016/j.heliyon.2017.e00379

are initial, and equilibrium concentrations of bacteria in solution, V (L) is the volume of bacteria solution, and w (g) is the weight of the dry composite adsorbent.

To obtain the concentration of the bacteria in mg/L, we first convert absorbance values obtained to g/L using Eq. (2) and subsequently to mg/L by multiplying the value obtained in g/L by 1000.

The equilibrium data obtained were fitted to five non-linear adsorption isotherm models: Freundlich, Langmuir, Brouer-Sotolongo, Sips and Jovanovic isotherms as described in section 2.6. All equilibrium plots were made using KyPlot® version 2.0 software.

2.6. Isotherm models

2.6.1. Freundlich isotherm

Freundlich isotherm model is based on equilibrium adsorption of adsorbate onto heterogeneous surfaces. This model is based on the assumption that the adsorption sites are evenly distributed exponentially with respect to heat of adsorption [30]. The model equation is given as:

$q_e = K_F C_e^{1/n_F}$ (1)

Where q_e is the maximum adsorption capacity of the bacteria (mg/g), n_F is the Freundlich isotherm constants related to adsorption intensity, K_f is the Freundlich isotherm constants related to adsorption capacity of the composite adsorbent (mg bacteria/g adsorbent) and C_e is the equilibrium concentration of the bacteria in solution (mg bacteria/L solution).

2.6.2. Brouers-Sotolongo isotherm

This isotherm is given by a deformed exponential (Weibull) function [31]. Its expression is given by:

$q_e = q_{max}(1\text{-}(1\text{-}\exp(\text{-}K_w C_e^{\alpha})))$ (2)

Where q_e is the maximum adsorption capacity of the composite adsorbent (mg bacteria/g adsorbent), q_{max} is the saturation value (mg bacteria/g adsorbent), $K_w = K_F/Q_{max}$ (where K_F is the low C_e Freundlich constant, for a given temperature), C_e is the equilibrium concentration of the bacteria in solution (mg bacteria/L solution), and α is a measure of the width of the sorption energy distribution and therefore of the energy heterogeneity of the sorbent surface.

2.6.3. Jovanovic isotherm

The assumption of this isotherm is similar to that considered by Langmuir isotherm which assumes a monolayer adsorption on the surface of the adsorbent. Jovanovic

http://dx.doi.org/10.1016/j.heliyon.2017.e00379

is represented by another approximation for monolayer localised adsorption without lateral interactions [32].

$q_e = q_m(1\text{-}e^{KjCe})$ (3)

Where q_e is the maximum adsorption capacity of the composite adsorbent (mg bacteria/g adsorbent), q_m is the maximum saturation value of the composite adsorbent (mg bacteria/g adsorbent), C_e is the equilibrium concentration of the bacteria in solution (mg bacteria/L solution), and k_j is Jovanovic isotherm constant.

2.6.4. Langmuir isotherm

Langmuir isotherm is valid for monolayer adsorption onto a surface containing a finite number of identical sites. The model assumes uniform energies onto the surface [33]. The Langmuir model is represented by the equation:

$q_e = (q_{max}K_LC_e)/(1 + K_LC_e)$ (4)

Where C_e is the equilibrium concentration of the bacteria in solution (mg bacteria/L solution), q_e is the amount of bacteria adsorbed per gram of the adsorbent at equilibrium (mg bacteria/g adsorbent), q_{max} is the maximum monolayer coverage (mg bacteria/g adsorbent), and K_L is the Langmuir isotherm constant (L/mg bacteria)

2.6.5. Sips isotherm

To circumvent the limitation of the increasing adsorbate concentration associated with the Freundlich isotherm model, the Sips isotherm combins the Langmuir and Freundlich expressions for modeling a heterogeneous adsorption system [34, 35, 36]. The mathematical expression for the isotherm is given below:

$q_e = (K_sC_e^{\beta s})/(1 + a_sC_e^{\beta s})$ (5)

Where K_s is the maximum adsorption capacity of the composite adsorbent (mg bacteria/g adsorbent), C_e is the equilibrium concentration of the bacteria (mg bacteria/L solution), β_s is the dimensionless heterogeneity factor, and a_s is Sips equilibrium constant (1/mg)

3. Results and discussion

3.1. Physicochemical analysis of composite adsorbents

3.1.1. X-ray diffraction

Fig. 1 presents the X-ray Diffraction profiles of raw Kaolinite and Ch-nHYCA$_{\mathbf{1:5}}$, Ch-zHYCA$_{\mathbf{1:2}}$ and Al-zHYCA$_{\mathbf{2:1}}$ composite adsorbents. The raw Kaolinite clay shows characteristic reflections for Kaolinite at 2θ 12.8° and 25.0° corresponding

http://dx.doi.org/10.1016/j.heliyon.2017.e00379

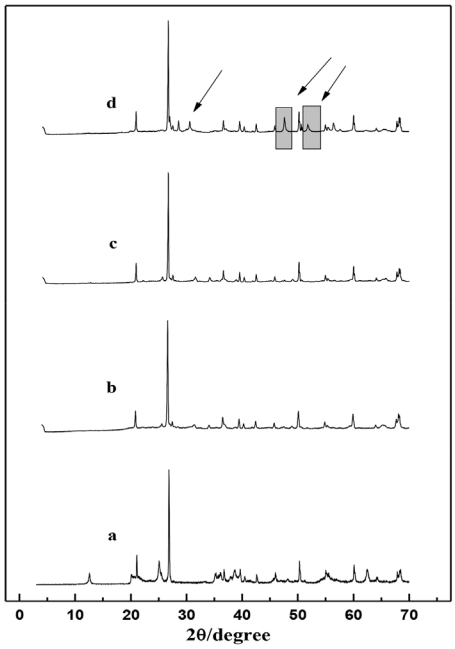

Fig. 1. X-ray diffraction of (a) Kaolinite (b) Ch-nHYCA$_{\mathbf{1:5}}$ (c) Ch-zHYCA$_{\mathbf{1:2}}$ (d) Al-zHYCA$_{\mathbf{2:1}}$ composite adsorbents.

to reflections from 001 and 002 [JCPDS card no. 29–1488] [37, 38] respectively. Other main reflections of Kaolinite observed were 2θ 35.5°, 38.7°, 45.9°, 55.4° and 62.3° [39].

Reflections corresponding to the quartz phase were also observed in the spectra of the raw Kaolinite (Fig. 1a) at 2θ 21.0°, 26°, 50.96°, and 68.2° [40, 41] [JCPDS card no. 46–1045] [42]. However, the three composites show patterns similar to that of kaolinite clay (Fig. 1b-d), thus confirming that the Kaolinite clay phase was still retained in the composite materials since they were not heated above 600 °C where Kaolinite is expected to undergo a phase transformation to metakaolin [43].

On the other hand, the significant difference between the spectra of the Al-zHYCA$_{\mathbf{2:1}}$ composite adsorbent and the raw Kaolinite is the appearance of new inflexions at 2θ 27-36° which contains peaks corresponding to silicate and sulphate phases [44]. There is also the disappearance of Kaolinite 001 and 002 reflections with the source of sulphate being from the Alum. Similarly, new phases analogous of ZnO and Kalininite (S, Zn) were observed at 2θ 36.3° [45], 47.3° [JCPDS card no. 36–1451] [46] and 51.8° [47] in the Al-zHYCA$_{\mathbf{2:1}}$ composite adsorbent. The spectra of the two chitosan modified composite adsorbents (Ch-zHYCA$_{\mathbf{1:2}}$, Ch-nHYCA$_{\mathbf{1:5}}$) did show similar new phases with same loss of both 001 and 002 reflections of Kaolinite like in Al-zHYCA$_{\mathbf{2:1}}$ composite adsorbent. It is not well understood what these new peaks are, but they imply that there were some changes

http://dx.doi.org/10.1016/j.heliyon.2017.e00379

in the crystalline structure of Kaolinite clay when it was used in preparing these composite adsorbents.

All of these indicate a change in the crystalline structure of the raw Kaolinite used in the preparation of these composites. The ZnO phase found in the composites is a result of the reaction between NaOH and $ZnCl_2$ used in the preparation of the composites as shown in the equation below.

$ZnCl_2 + 2NaOH \rightarrow ZnO + 2NaCl + H_2O$ (3)

3.1.2. Fourier transformed infrared analysis

The chemical functionalities of prepared composite adsorbents were analyzed using the Fourier Transformed Infrared Spectroscopy (FT-IR). Fig. 2 shows the FT-IR spectra of the prepared composites.

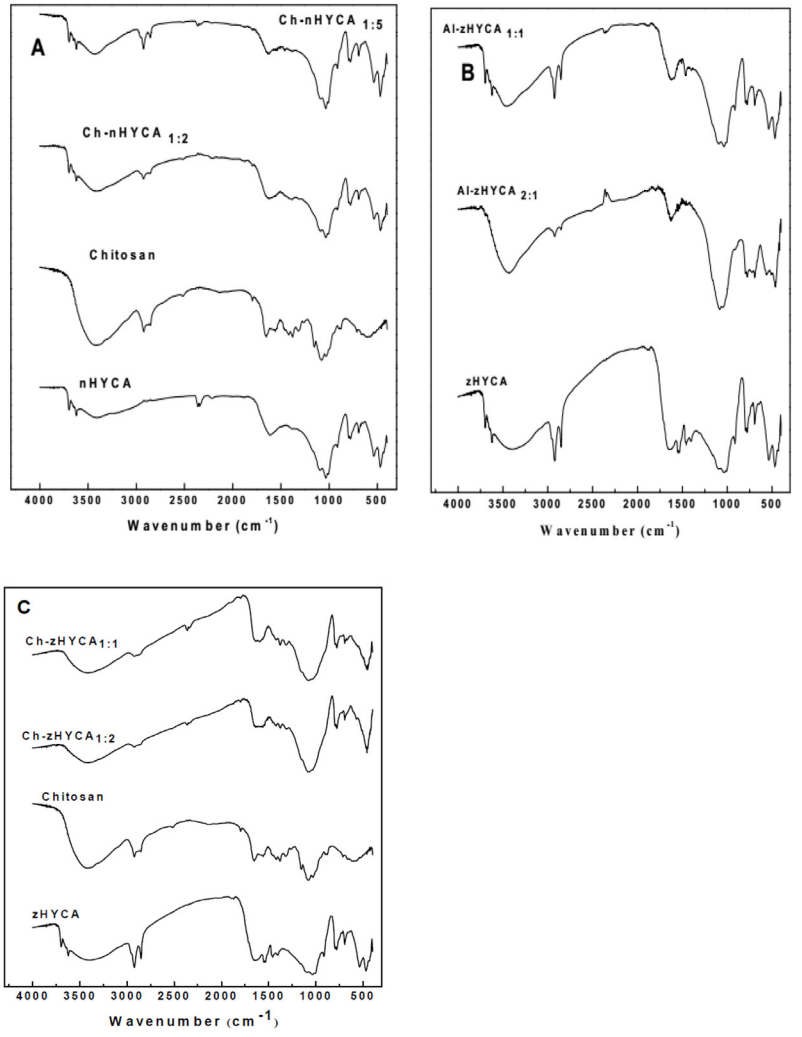

Fig. 2. Fourier Transformed-Infrared Spectra of (A) Ch-nHYCA (B) Al-zHYCA (C) Ch-zHYCA composite adsorbents.

http://dx.doi.org/10.1016/j.heliyon.2017.e00379

In a previous work done by Unuabonah, et al. [23] the FT-IR spectra of Kaolinite clay and *Carica papaya* seeds were discussed. The raw Kaolinite clay showed characteristic bands at 3697 cm^{-1} and 3622 cm^{-1} which correspond to the inner octahedral structure of Al-O-H bonds. The bands observed at 3441 $cm^{-1,}$ and 1627 cm^{-1} were suggested to be the -O-H stretching and bending vibrations respectively. The bands at 1097 cm^{-1} and 912 cm^{-1} were assigned the Si-O and Al-OH in plane bending vibrations respectively. The peaks in the range 1200–400 cm^{-1} correspond to the presence of Si-O stretching and bending vibrations [48]. For the *Carica papaya* seeds, a strong peak indicating the presence of phenolics and carboxylic -OH stretching vibration was found around 3402 cm^{-1}, while the broad band between 3480 cm^{-1} and 3440 cm^{-1} correspond to the vibrational frequency of -N-H band [49].

Fig. 2A shows the FT-IR spectra of hybrid clay prepared with NaOH (nHYCA), chitosan and chitosan modified hybrid clay in the ratios 1:2 and 1:5 respectively. The FT-IR spectrum of nHYCA composite adsorbent have been well discussed in our previous article [23]. The FT-IR spectra of the chitosan shown in Fig. 2A, the -OH stretching vibration was observed as a broad peak in the range from 3750–3000 cm^{-1}, thus overlapping with the -N-H stretching vibration frequency [50]. Absorption bands in the region of 1680–1480 cm^{-1} correlates with vibrations of carbonyl bonds (-C=O) of an amide group, CONHR (secondary amide) and those of protonated amide group which occurs at ca. 1574 cm^{-1} [51]. Vibrational frequencies in the range 1160–1000 cm^{-1} were due to the vibrations from -C-O groups [52]. Specifically, the peak around 1150 cm^{-1} corresponds to the vibrations of -C-O in an oxygen bridge resulting from deacetylation of chitosan, while the bands within 1080–1025 cm^{-1} are assigned to the vibrations of -C-O-, -C-O-C- and CH_2OH in ringed systems [53]. The peak at ~890 cm^{-1} correlates to the wagging vibration of the saccharide structure of chitosan [53]. The FT-IR spectra of the composite adsorbents shows that there is a narrowing and an increase in the intensity of the broad peak in the 3750–3000 cm^{-1} range especially with increased amount of chitosan in the composite mix [50, 54]. Although the ratio of chitosan to HYCA was decreased from 1:3 to 1:5 (Fig. 2A), there was no observable change in the spectra except that there was an increase in the intensity of 2920 cm^{-1} and 2853 cm^{-1} peaks (asymmetric and a symmetric -C-H stretch of $-CH_2$ [55] respectively) indicating a significant presence of -C-H in the Ch-nHYCA composite adsorbents. The 3697 cm^{-1} and 3622 cm^{-1} peaks which correspond to the inner octahedral structure of Al-O-H bonds from the clay mineral are still visible despite the modification with chitosan. In addition, the FT-IR spectra of the composite adsorbents shows that there is a narrowing of the broad peak in the 3750–3000 cm^{-1} range especially with increased portion of the hybrid clay in the composite mix. This could be associated with reduced freedom of motion of interfacial and polar headgroups of chitosan [56]. However, there is difference between the shape

http://dx.doi.org/10.1016/j.heliyon.2017.e00379

of this broad band changed in the modified samples and that of nHYCA sample (Fig. 2A). This suggests that the inner hydroxyl -OH groups of the Kaolinite clay mineral may be involved in the modification process.

Fig. 2B shows the FT-IR spectra of the synthesized microwave assisted Zn-doped hybrid clay composite adsorbent (zHYCA) and the alum modified zHYCA (Al-zHYCA$_{\mathbf{1:1}}$, Al-zHYCA$_{\mathbf{2:1}}$). The spectra of zHYCA showed peaks that are characteristics of both Kaolinite clay and papaya seed as described by Unuabonah et al. [23]. However, the presence of -C-H (2922 cm^{-1}) in the papaya seed and Si-O bending vibration (1097 cm^{-1}) of the Kaolinite clay suggests a possible interaction between the Kaolinite clay and papaya seed. The change in the shape of the peak between 3600–3100 cm^{-1} in the Al-zHYCA adsorbents when compared with zHYCA adsorbent suggests an interaction between the alum and the zHYCA composite. The shift in the Si-O vibration for Kaolinite from 1097 cm^{-1} [23] to 1038 cm^{-1} for Zn-doped HYCA, 1058 cm^{-1} for Al-zHYCA$_{\mathbf{1:1}}$ and 1083 cm^{-1} for Al-zHYCA$_{\mathbf{2:1}}$ composite adsorbent is an indication of a chemical interaction between Al/Fe (from the commercial Alum) and Si-O. Increasing the ratio of aluminium in the composites from 1 to 2 tend to reduce the intensity of the 2922 cm^{-1} peak of -C-H stretching vibration (Fig. 2B). The change in the shape of the -O-H bending vibration with increasing Al may be attributed to the presence of a new type of -O-H which is likely a contribution from Al.

Fig. 2C shows the FT-IR spectra for chitosan modified Zn-doped HYCA adsorbent prepared via the microwave-assisted technique. The FT-IR of the composite adsorbents shows similar patterns with only a slight shift in the position of the bands due to the presence of chitosan in the composites. On changing the ratio of chitosan:zHYCA in the composite adsorbent from 1:1 to 1:2, there is an observed reduction in the intensity of -C-H asymmetric and a symmetric stretch of $-CH_2$ usually found around 2920 cm^{-1} and 2853 cm^{-1} [55]. Broadening of the -C=O stretching vibration of secondary amine in chitosan at 1647 cm^{-1} was observed in both Ch-zHYCA$_{\mathbf{1:1}}$ and Ch-zHYCA$_{\mathbf{1:2}}$ composite adsorbents with a ZnO peak at 459 cm^{-1} (Fig. 2C).

However, the 1:1 composite adsorbents showed very poor efficiency in the removal of bacteria from water during a preliminary study with these adsorbents. They are, therefore, no longer referred to in the course of discussion in this article.

3.1.3. Surface morphology analysis

Fig. 3 shows the scanning electron microscope images of prepared composite adsorbents, raw Kaolinite and *Carica papaya* seeds. The flaky nature of the Kaolinite clay surface is observed to have undergone significant alteration due to the chemical and thermal treatment which the materials have been subjected to. The morphology of Ch-nHYCA$_{\mathbf{1:5}}$ adsorbent shows a homogeneous composite

http://dx.doi.org/10.1016/j.heliyon.2017.e00379

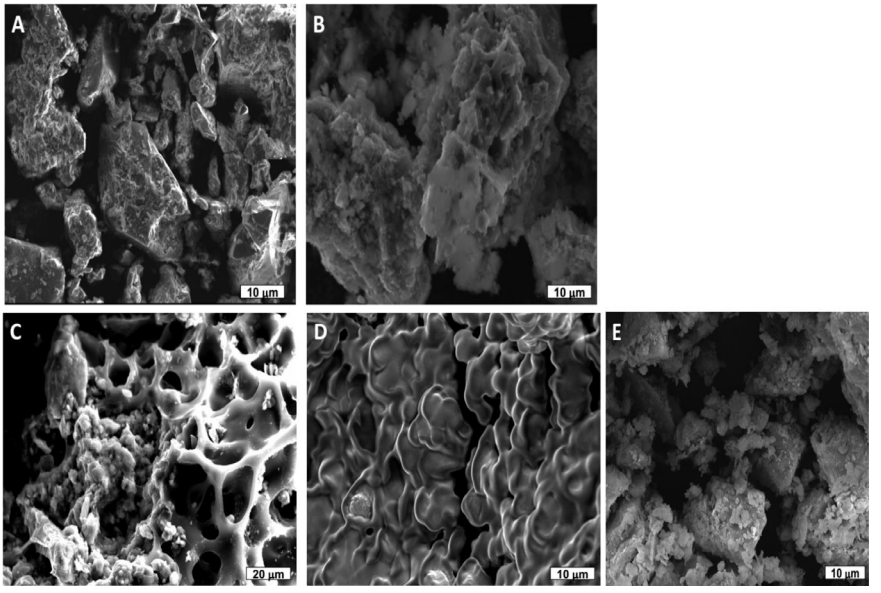

Fig. 3. Scanning Electron Microscopy Images of (A) Ch-nHYCA$_{\mathbf{1:5}}$ (B) Al-zHYCA$_{\mathbf{2:1}}$ (C) Ch-zHYCA$_{\mathbf{1:2}}$ composite adsorbents (D) carica papaya seed and (E) Raw Kaolinite.

with particle structure that is irregular and different from those of the originating Kaolinite clay (Fig. 3A). The particles of Al-zHYCA$_{\mathbf{2:1}}$ composite adsorbent appear lumped together (Fig. 3B) while those of Ch-zHYCA$_{\mathbf{1:2}}$ show a heterogeneous structure (Fig. 3C). To confirm the presence of certain elements in Ch-nHYCA$_{\mathbf{1:5}}$, Ch-zHYCA$_{\mathbf{1:2}}$, and Al-zHYCA$_{\mathbf{2:1}}$ composite adsorbents, they were analyzed using the elemental mapping mode of the Scanning Electron Microscopy equipment.

Fig. 4a shows the elemental mapping image and a cross-section of the elemental distribution in Ch-zHYCA$_{\mathbf{1:2}}$ composite adsorbent. The image confirm the presence of Zn (from the $ZnCl_2$ used for activation) and C (from chitosan) indicating the successful modification of the HYCA material with Chitosan. The elemental mapping images also showed the presence of Ti, Fe, K, and Ca (not shown) which are elements typically present in Kaolinite clay in trace amounts [57]. Zn in the composite material appears not to be evenly distributed in the sample while carbon is localized in certain areas of the sample.

However, with Ch-nHYCA$_{\mathbf{1:5}}$ composite adsorbent, the presence of carbon (C) evenly distributed on the surface of the material with a few dense spots of C (Fig. 4b) confirms the success of the modification of nHYCA with chitosan.

For the alum modified zHYCA composite (Al-zHYCA$_{\mathbf{2:1}}$), the presence of sulphur (S) and potassium (K) both confirmed the presence of Alum [$KAl(SO_4)_2.12H_2O$] in the bulk of the composite adsorbent (Fig. 4c). The presence of Zn also confirms the incorporation of the activating agent (Zn salt) into the bulk of the composite adsorbent.

http://dx.doi.org/10.1016/j.heliyon.2017.e00379

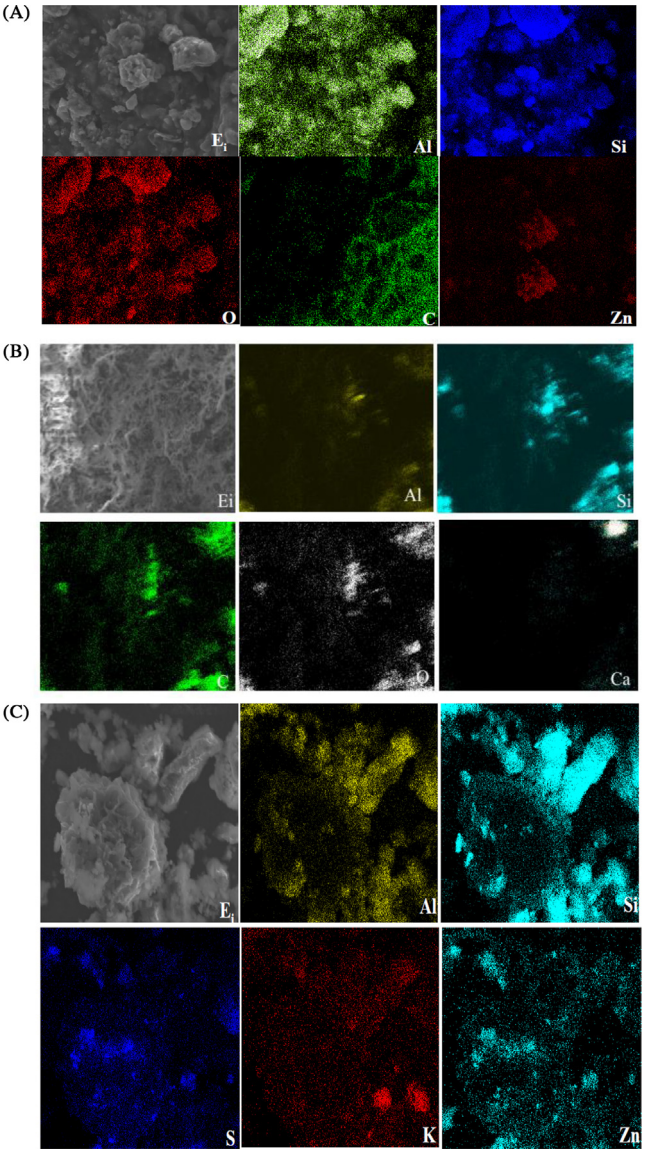

Fig. 4. Elemental mapping images (Ei) and surface distribution of some elements in (A) Ch-zHYCA$_{1:2}$ composite adsorbent. (B) Ch-nHYCA$_{1:5}$ composite adsorbent. (C) Al-zHYCA$_{2:1}$ composite adsorbent.

Table 1 shows the metal composition of the various composite adsorbents obtained via the Energy Dispersive X-ray. The data in Table 1 was arrived at from the sum of the various data from each site on a sample. The table suggests that Ch-nHYCA$_{1:5}$ composite adsorbents contain more oxygen than either Ch-zHYCA$_{2:3}$ and Al-zHYCA$_{2:1}$ composite adsorbents. The element, P, in both Ch-zHYCA$_{1:3}$ and Al-zHYCA$_{2:1}$ composite adsorbents appears to be leached out by NaOH during the preparation of Ch-nHYCA$_{1:5}$ composite adsorbent. Although, the elements P and K are from *Carica papaya* seeds [58, 59], Ca, Ti and Fe are from Kaolinite clay, they appear to be leached by the preparation process for Ch-

http://dx.doi.org/10.1016/j.heliyon.2017.e00379

Table 1. Elemental Composition of Composites by Atomic Percent (%).

Element	Ch-zHYCA$_{1:2}$	Ch-nHYCA$_{1:5}$	Al-zHYCA$_{2:1}$
O	37.6	50.87	47.37
Mg	0.56	1.11	-
Al	7.86	9.93	10.95
Si	34.03	25.08	23.97
P	0.79	-	0.73
Cl	0.87	-	0.68
K	3.05	1.43	1.04
Ca	1	4.48	0.85
Ti	1.24	1.56	0.44
Fe	1.76	5.52	0.82
Zn	8.29	-	6.06
S	-	-	7.04

zHYCA$_{1:2}$ and Al-zHYCA$_{2:1}$ composite adsorbents. The absence of Zn and Cl in Ch-nHYCA$_{1:5}$ composite adsorbent confirms that $ZnCl_2$ was not used in its preparation. The low content of Al in the composite even when zHYCA was modified with commercial alum (Table 1) suggests that Al was not significantly doped into zHYCA as expected.

3.1.4. pH point of zero charge

Fig. 5 shows the pH_{pzc} curves for the composite adsorbents. The pH point of zero charge for the zHYCA, Ch-zHYCA$_{1:2}$, Ch-zHYCA$_{1:1}$ is 5.81, 7.44 and 7.17 respectively (Fig. 5). This shows that the modification of the zHYCA with chitosan resulted in an increase in the pH_{pzc} of the material. This is in agreement with the findings by Hatice et al. [60], who reported an increase in the pH_{pzc} of a Kaolinite clay material from 2.8 to 5.8 when coated with chitosan.

The pH_{pzc} of zHYCA composite adsorbents increased from 5.81 in zHYCA to 6.64 in Al-zHYCA$_{1:1}$ and 6.91 in Al-zHYCA$_{2:1}$ composite adsorbents (Fig. 5B). This small shift in pHpzc is as a result of the presence of alum which is basic [61].

For the chitosan doped nHYCA, the Ch-nHYCA$_{1:1}$ gave a pH_{pzc} value of 7.58, the same value reported by Unuabonah et al. [23] for NaOH-activated hybrid clay composite adsorbent (nHYCA). The pH_{pzc} of the nHYCA is increased to 8.45 on increasing the amount of nHYCA in the composite adsorbent to 5 (Ch-nHYCA$_{1:5}$). The small increase in the pH_{pzc} of the Chitosan modified materials confirms that there is an increase in basic groups present on the surface of the composite material due to delocalized π electrons activated via heating and the presence of oxygen containing functional groups acting as Lewis bases [23], [62, 63].

http://dx.doi.org/10.1016/j.heliyon.2017.e00379

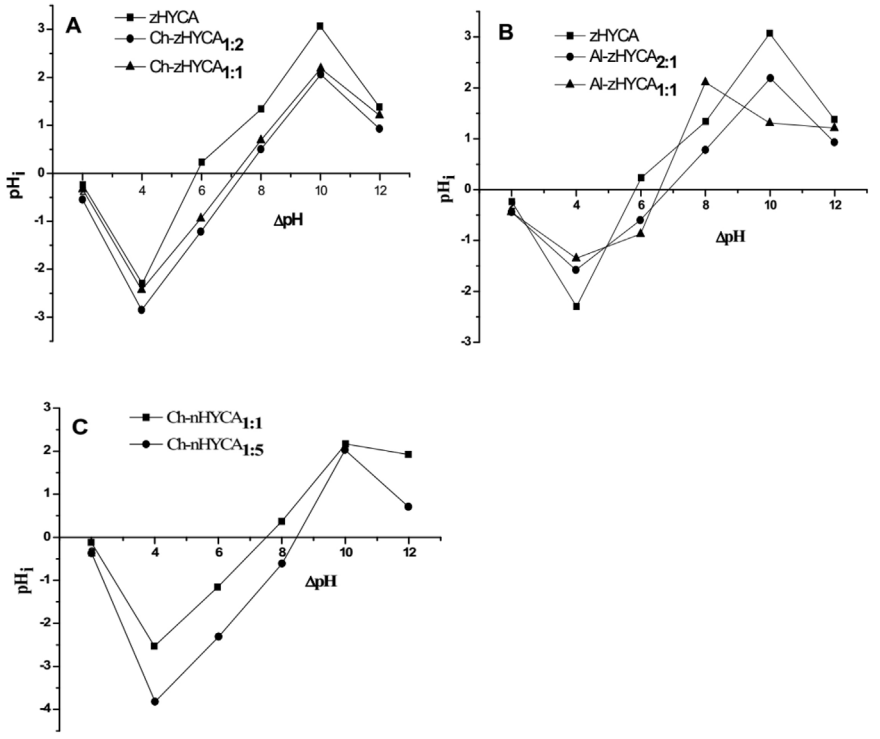

Fig. 5. pH_{pzc} curve for (A) zHYCA, Ch-zHYCA$_{1:1}$, Ch-zHYCA$_{1:2}$ (B) zHYCA, Al-zHYCA$_{1:1}$, Al-zHYCA$_{1:2}$ (C) Ch-nHYCA$_{1:5}$, Ch-nHYCA$_{1:1}$ composite adsorbents.

3.2. Efficiency of removal evaluation

An initial experiment was carried out to determine the anti-bacteria activity of the prepared composite adsorbents (Ch-zHYCA, Ch-nHYCA, and Al-zHYCA) measured against time using a concentration of 52 mg/L (1.3×10^7 cfu/mL) for *E. coli*, 89 mg/L (2.3×10^7 cfu/mL) for *V. cholerae* and 67 mg/L (1.7×10^7 cfu/mL) for *S. typhi*. It was observed that the most efficient composite adsorbent for the removal of these bacteria was Ch-nHYCA$_{1:5}$ with a maximum adsorption percentage removal value of 17.7% (4.07×10^6 cfu/mL) for *V. cholerae* after 120 min, 15.0% (1.95×10^6 cfu/mL) for *E. coli* after ~180 min and 19.1% (3.25×10^6 cfu/mL) for *S. typhi* after 270 min (Fig. 6A-C).

Although these percentage removals appear very low, yet they are very significant when compared with the alert/action limit of 500 cfu/mL for these bacteria in water [64]. In support of this, an experiment was carried out using a lower concentration of *E. coli* (10^3 cfu/mL) in solution with 2 g of the Ch-nHYCA$_{1:5}$ composite adsorbent (which gave the best result as seen from Fig. 6) at a flow rate of 8 mL/min. It kept the amount of *E. coli* in solution at zero for up to 10 h after which some small amounts of *E. coli* between 10–250 cfu/mL were observed up till 16 h.

http://dx.doi.org/10.1016/j.heliyon.2017.e00379

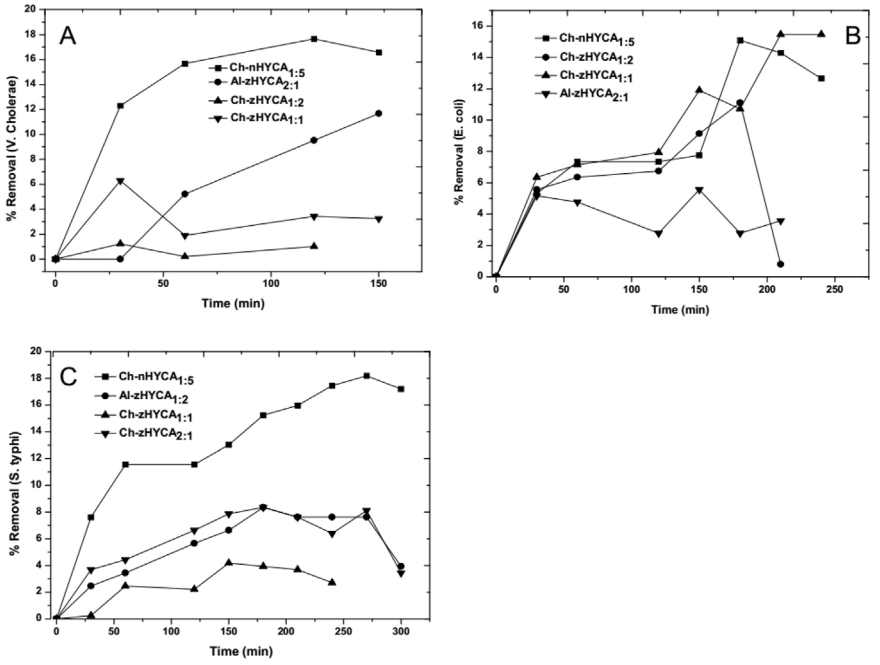

Fig. 6. Percentage removal of (A)*V. cholerae* (B) *E. coli*, and (C) *S. typhi by various hybrid clay composite adsorbents.*

From Fig. 6, it was observed that when nHYCA, Al-zHYCA$_{\mathbf{1:1}}$, Ch-zHYCA$_{\mathbf{1:1}}$ and Ch-nHYCA$_{\mathbf{1:3}}$ composite adsorbents were initially used to remove these bacteria from contaminated water, there was no significant removal efficiency (nHYCA and Al-zHYCA$_{\mathbf{1:1}}$ results not shown as they showed the worst efficiencies). However, with the modified composite adsorbents as shown in Fig. 6 (Ch-zHYCA$_{\mathbf{1:2}}$, Ch-nHYCA$_{\mathbf{1:5}}$, and Al-zHYCA$_{\mathbf{2:1}}$) the quantity of bacteria removed from contaminated water increased with time especially within the first 50 min of the experiment (which is in contrast with ~8 h as reported by Papaphilippou, et al. [10]).

3.3. Adsorption capacity study

Going by the removal efficiency evaluation as shown in Fig. 6 it is observed that Ch-nHYCA$_{\mathbf{1:5}}$ composite adsorbent shows the best efficiency in the removal of these enteric bacteria throughout all the time used for the study. Subsequently, equilibrium adsorption of these enteric bacteria (*E. coli*, *S. typhi* and *V. cholera*) was studied using Ch-nHYCA$_{\mathbf{1:5}}$ composite adsorbent. Adsorption isotherm models are non-linear curves depicting the adsorption process at constant pH and temperature. Fitting of experimental isotherm data to known mathematical adsorption model plots provides a route for evaluating and predicting the adsorption capacity of an adsorbent. Determination of the appropriate equilibrium adsorption isotherm can help in the evaluation of adsorption capacity of

http://dx.doi.org/10.1016/j.heliyon.2017.e00379

adsorbents, adsorption mechanism pathways, process optimization and efficient adsorption system design [65].

In this study, five isotherm models were employed: Langmuir, Freundlich, Brouers-Sotolongo (BWI), Jovanovic and Sips isotherms. The non-linear isotherm model fits for the adsorption of *E. coli*, *V. cholerae* and *S. typhi* onto Ch-nHYCA$_{\mathbf{1:5}}$ composite adsorbent are shown in Fig. 7A-C and results for the parameters for the various models are shown in Table 2.

Although the Freundlich model best described data from *E. coli* and *V. cholerae* adsorption based on r^2 values (Table 2), its K_F values underestimated the experimental maximum adsorption capacity of Ch-nHYCA$_{\mathbf{1:5}}$ composite adsorbent to remove these bacteria from solutions (*E. coli* 0.24 mg/g = 1.85×10^5 cfu/mL (6.17×10^7 cfu/g) and *V. cholerae* 0.22 mg/g = 1.69×10^5 cfu/mL (5.63×10^7 cfu/g) as against the experimental values of 3.25×10^6 cfu/mL (1.08×10^9 cfu/g) for *E. coli* and 1.95×10^6 cfu/mL (6.50×10^8 cfu/g) for *V. cholerae* as earlier discussed). The Brouers-Sotolongo model which ranks next to the Freundlich model, appropriately describes the maximum adsorption capacity (q_{max}) of Ch-nHYCA$_{\mathbf{1:5}}$ composite adsorbent for the adsorption of *E. coli* as 103.07 mg/g (7.93×10^7 cfu/mL = 2.64×10^{10} cfu/g) and *V. cholerae* as 154.18 mg/g (1.19×10^8 cfu/mL = 3.97×10^{10} cfu/g). This is an indication that the surface of Ch-nHYCA$_{\mathbf{1:5}}$ is

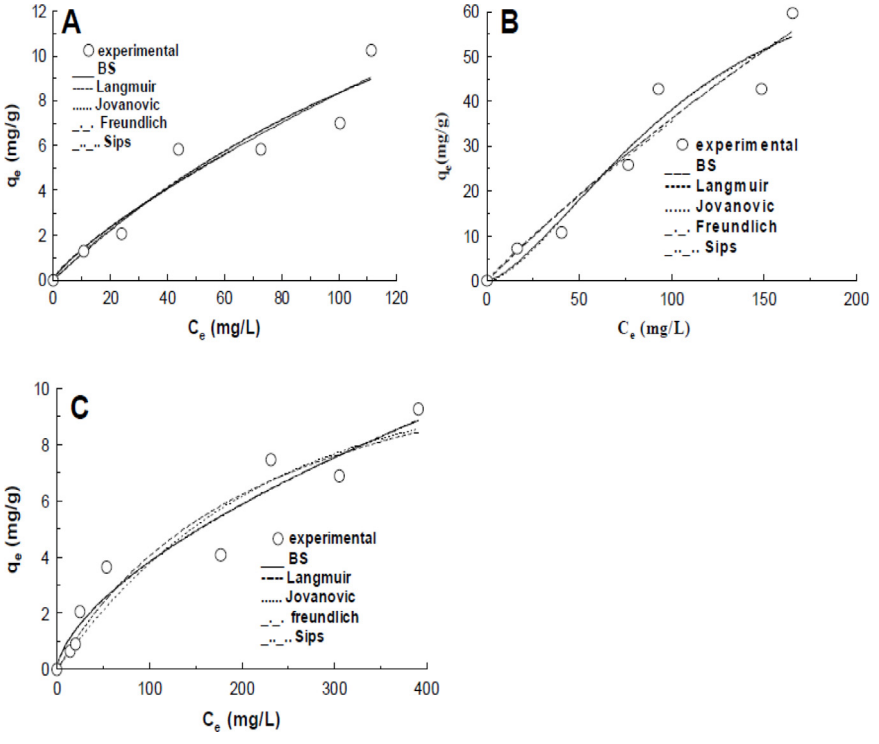

Fig. 7. Non-linear curves for the equilibrium adsorption capacity plots for (A) *E. coli* (b) *S. typhi* (C) *V. cholerae* on Ch-nHYCA$_{\mathbf{1:5}}$ composite adsorbent.

http://dx.doi.org/10.1016/j.heliyon.2017.e00379

Table 2. Isotherm parameters for *enteric bacteria* adsorption on Ch-nHYCA$_{1:5}$ adsorbent.

Isotherm Model	*E. coli*	*V. Cholerae*	*S. typhi*
Freundlich			
K_F $[(mg/g)(L/mg)^{1/n}]$	0.24	0.22	0.54
n_F	1.28	1.62	1.1
r^2	0.9209	0.9388	0.9339
Error	1.25	0.78	39.03
Langmuir			
q_{max} *(mg/g)*	25.62	13.54	308.24
K_L *(l/mg)*	0.0048	0.0042	0.0013
r^2	0.9194	0.9236	0.9355
Error	1.28	0.97	38.07
Jovanovic			
q_{max} (mg/g)	15.69	10.27	165.77
K_J	0.0076	0.0046	0.0024
r^2	0.9185	0.9166	0.9356
Error	1.3	1.06	38.03
Sips			
q_{max} *(mg/g)*	128.14	177.66	83.65
a_s	0.0038	2.45 × 10-5	0.0089
b_s	0.808	0.63	1.6
r^2	0.9208	0.9385	0.9393
Error	1.57	0.91	44.83
Brouers-Sotolongo			
q_{max} *(mg/g)*	103.07	154.18	64.35
K_w *(l/mg)*	0.002	0.0014	0.0011
α	0.8	0.63	1.44
r^2	0.9208	0.9386	0.9389
Error	1.57	0.91	45.07

heterogeneous with patches of active sites with equal energy [66]. However, based on the r^2 values, the Sips model best described the adsorption data for the adsorption of *S. typhi* by Ch-nHYCA$_{1:5}$ composite adsorbent from aqueous solution with an estimated maximum adsorption capacity of 83.65 mg/g (6.43×10^7 cfu/mL = 2.14×10^{10} cfu/g). These all exceed the value of 1.5×10^6 cfu/mL for zHYCA in our recent study[25] indicating the better efficiency of the new composite adsorbent. Although, this model (Sips) does describe a heterogeneous adsorbent surface, yet at high concentration of the adsorbate, it forecast a

http://dx.doi.org/10.1016/j.heliyon.2017.e00379

monolayer adsorption capacity [35] which best describes our result for the adsorption of *S. typhi* by Ch-nHYCA$_{\mathbf{1:5}}$ composite adsorbent in this study.

However, the n_F values from the Freundlich model which are in the range of 1 to 10 is a proof of the favourable adsorption of the bacteria [67]. Furthermore, the n_F values suggests that the interaction between these bacteria and Ch-nHYCA$_{\mathbf{1:5}}$ composite adsorbent is a chemisorption process with the surface of the adsorbent being heterogeneous in nature [32].

The adsorption capacities of Ch-nHYCA$_{\mathbf{1:5}}$ composite adsorbent (from Brouers-Sotolongo models) for the removal of these enteric bacteria from water are higher than those of acid-modified clinoptilolite (20–25 mg/g) [68] and commercial activated carbon (8.0×10^6 cfu/mL) [69]. The adsorption capacities of Ch-nHYCA$_{\mathbf{1:5}}$ composite adsorbent for these enteric bacteria compares favourably with values obtained by Camper et al. [70] who measured 5×10^7 cfu of bacteria/g Granular Activated Carbon (GAC), Niemi et al. [71] who obtained 6×10^7 to 10^8 cfu of bacteria/g GAC dry weight and Borkowski et al., [72] that reported values between 0.22 and 8.26×10^7 cfu/g SiC Nanofibers, SiC Nanorods and micrometric SiC. This suggests the strong potential of Ch-nHYCA$_{\mathbf{1:5}}$ composite adsorbent for the removal of these enteric bacteria from water more so that the alert and action levels of these bacteria in natural water do not exceed 500 cfu/mL [64].

Fig. 8 shows the FT-IR spectra of unloaded and bacteria-loaded Ch-nHYCA$_{\mathbf{1:5}}$ composite adsorbent. There is a strong contribution of Amide I band from proteins of these bacteria such that the peak at 1628 cm^{-1} [73], shows very strong intensity with the adsorption of these gram-negative bacteria [55, 74]. The shape of this

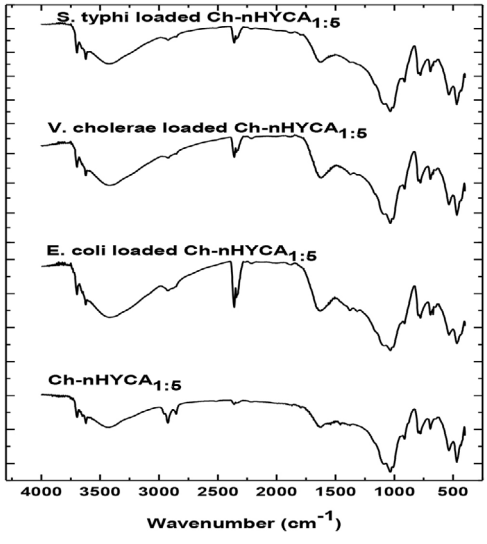

Fig. 8. Fourier-Transformed Infrared Spectroscopy of unloaded and bacteria-loaded Ch-nHYCA$_{\mathbf{1:5}}$ composite adsorbent.

http://dx.doi.org/10.1016/j.heliyon.2017.e00379

band in the unloaded bacteria is different from that on the bacteria loaded composites. Similarly, the -O-H stretching vibration of Ch-nHYCA$_{\mathbf{1:5}}$ composite adsorbent at 3418 cm^{-1} show strong intensity with the adsorption of these bacteria on its surface. The change in the intensity of the double peak at 2366 cm^{-1} in the bacteria-loaded composite adsorbents representing O = C − O vibration could indicate contribution of this functionality from cell wall component of the bacteria [75, 76]. All of these points to the fact that these test bacteria used in this study (*E. coli, V. cholerae and S. typhi*) were indeed adsorbed by the composite adsorbent.

An explanation for the bacteriostatic mechanism of Ch-nHYCA$_{\mathbf{1:5}}$ composite adsorbent is not yet fully understood. However, the pH_{pzc} could be used to give some explanation. The pH_{pzc} of Ch-nHYCA$_{\mathbf{1:5}}$ composite adsorbent is 8.45. Carrying out the adsorption of these bacteria (*E.coli*, *S. typhi* and *V. cholerae*) at a pH of ca. 6.1 suggest that the removal of these bacteria from solutions could be by electrostatic interaction since below the pHpzc, the composite adsorbent (Ch-nHYCA$_{\mathbf{1:5}}$) is expected to be positively charged. Chitosan presents positive charges density when the pH is lower than its pKa (6.5). In this case, the protonated amine groups (NH_3^+) at the C2 position in the glucose monomer of chitosan chains allow the formation of a polycationic structure, which can interact with anionic compounds and macromolecular structures of gram-negative bacteria [77, 78, 79]. It is, thus, believed that this kind of interaction triggers secondary cellular effects such as destabilization and subsequent disruption of bacterial membrane function via unknown mechanisms thereby compromising the membrane barrier function or causing cell lysis [80, 81]. Furthermore, it is expected that the ZnO will also play a role in the removal of these bacteria from solution via electrostatic interaction since below the isoelectric point of ZnO (pH 9–10), ZnO becomes $ZnOH^+$ [82] for all zHYCA composite adsorbents. Nonetheless, it has been suggested that several other factors can be responsible for the antimicrobial nature of Chitosan including the polymer molecular weight and degree of acetylation [83], hydrophobicity and size of adsorbent, which could influence the adsorption of these bacteria onto an adsorbent [9].

4. Conclusion

This study demonstrated the treatment of microbial polluted water by adsorption technique using new modified hybrid clay composite adsorbents. Characterisation tests confirmed successful modification of hybrid clay composite with chitosan, $ZnCl_2$ and commercial Alum. The results obtained show that chitosan modified hybrid clay (Ch-nHYCA$_{\mathbf{1:5}}$) adsorbent, an easily synthesized composite material, exhibited the highest microbial removal efficiency from the contaminated water. The isotherm study indicated that adsorption of bacterial occurred on the different adsorption sites on the external surface of the Ch-nHYCA$_{\mathbf{1:5}}$ adsorbent. Interestingly, bacterial adsorption was deemed to be complete in reasonable time, unlike most literature reports where adsorption took longer time. Its adsorption

http://dx.doi.org/10.1016/j.heliyon.2017.e00379

capacity does compare favourably with commercial Granular Activated Carbon and Nanostructured SiC. This adsorbent could be further developed for use in Point-of-Use systems for households.

The sustainability of the Ch-nHYCA$_{\mathbf{1:5}}$ composite adsorbent material stems from the fact that chitosan can be easily sourced from snail shells and other marine waste while Kaolinite is found in huge deposits around some developing countries including Africa. *Carica papaya* is an agro-waste which can easily be sourced especially in West Africa. The entire preparation process for the composite adsorbent is simple and easy to transfer.

Declarations

Author contribution statement

Emmanuel I. Unuabonah: Conceived and designed the experiments; Analyzed and interpreted the data; Wrote the paper.

Christina Guenter, Scott O. Fayemi: Contributed reagents, materials, analysis tools or data.

Matthew O. Kolawole: Conceived and designed the experiments; Wrote the paper.

Martins O. Omorogie, Olalekan C. Olatunde: Performed the experiments; Wrote the paper.

Adewale Adewuyi: Analyzed and interpreted the data.

Chukwunonso P. Okoli: Conceived and designed the experiments; Analyzed and interpreted the data.

Foluso O. Agunbiade: Conceived and designed the experiments; Wrote the paper.

Andreas Taubert: Analyzed and interpreted the data; Contributed reagents, materials, analysis tools or data;

Funding statement

This work was supported by The World Academy of Science (TWAS) with a grant (10-215 RG/CHE/AF/AC_G-UNESCO FR: 324028613).

Competing interest statement

The authors declare no conflict of interest.

Additional information

No additional information is available for this paper.

http://dx.doi.org/10.1016/j.heliyon.2017.e00379

References

[1] C.H. Weng, C.P. Huang, Adsorption Characteristics of Zn (II) from Dilute Aqueous Solution by Fly ash, Colloid. Surf. A 274 (1-3) (2004) 137–143.

[2] A. Imran, New Generation Adsorbent For Water Treatment, Chem. Rev. 112 (10) (2012) 5073–5091.

[3] C. Escobar, A. Randall, J. Taylor, Bacterial growth in distribution systems: effect of assimilable organic carbon and biodegradable dissolved organic carbon, Environ. Sci. Technol. 35 (2001) 3442–3447.

[4] I. Majsterek, P. Sicinska, A. Tarczynska, M. Zalewski, Z. Walter, Toxicity of microcystin from cyanobacteria growing in a source of drinking water, Comp. Biochem. Physiol. C Toxicol. Pharmacol. 139 (2004) 175–179.

[5] S. Pfaller, Innovative Methods For Determining the Microbiological Quality of Drinking Water, Elsevier, 2014.

[6] UNICEF, Water, Sanitation, and Hygiene Annual Report, UNICEF, New York, 2009.

[7] M. Craun, G. Craun, R. Calderon, M. Beach, Waterborne Outbreaks Reported in the United States, J. Water Health 4 (2006) 19–30.

[8] A.S. Biryukov, V.F. Gavrikov, O. Nikiforova, V.A. Shcheglov, New Physical methods of disinfection of water, J. Russ. Laser Res. 26 (2005) 13–25.

[9] H.-M. Moon, J.-W. Kim, Carbon Nanotube Clusters as Universal bacterial Adsorbents and Magnetic Separation Agents, Biotechnol. Prog. 26 (2009) 179–185.

[10] P. Papaphilippou, I. Vyrides, F. Mpekris, T. Stylianopoulos, C.A. Papatryfonos, C.R. Theocharis, et al., Evaluation of novel, cationic electrospun microfibrous membranes as adsorbents in bacteria removal, RSC Adv. 5 (2015) 67617–67629.

[11] M.J. Nieuwenhuijsen, J. Grellier, R. Smith, N. Iszatt, J. Bennett, N. Bset, et al., The Epidemology and possible mechanisms of Disinfection by-products in Drinking Water, Phil. Trans. R. Soc. A 367 (2009) 4043–4076.

[12] C. Xi, Y. Zhang, C.F. Marrs, W. Ye, C. Simon, B. Foxman, et al., Prevalence of Antibiotic Resistance in Drinking Water Treatment and Distribution Systems, Appl. Environ. Microbiol. 75 (17) (2009) 5714–5718.

[13] Q.-B. Yuan, M.-T. Guo, J. Yang, Fate of Antibiotic Resistant Bacteria and Genes during Wastewater Chlorination: Implication for Antibiotic Resistance Control, PLoS One 10 (3) (2015) e0119403.

http://dx.doi.org/10.1016/j.heliyon.2017.e00379

[14] R. Nassar, E. Browne, J. Chen, A. Klibanov, Removing human immune deficiencyvirus (HIV) from human blood using immobilized heparin, Biotechnol. Lett. 34 (2012) 853–856.

[15] K. Pankaj, R. Tyagi, V. Smriti, K. Dharmendra, T. Shruti, Nanomaterials Use in Wastewater Treatment. International Conference on Nanotechnology and Chemical Engineering (ICNCS'2012) Bangkok, Thailand, (2012) .

[16] N. Savage, M.S. Diallo, Nanomaterials and Water Purification: Opportunities and Challenges, J. Nanopart. Res. 7 (2005) 331–342.

[17] H. Zhang, Application of Silvernanoparticles in Drinking Water Purification [PhD], University of Rhode Island, USA, 2013.

[18] G. Ghasemzadeh, M. Momenpour, F. Omidi, M.R. Hosseini, M. Ahani, A. Barzegari, Applications of Nanomaterials in Water treatment and Environmental remediation, Front. Environ. Sci. Eng. 8 (2014) 471–482.

[19] M.C. Stensberg, Q. Wei, E.S. McLamore, D.M. Porterfield, A. Wei, S. Sepulveda, Toxicological Studies on Silver Nanoparticles: Challenges and Opportunities in assessment, monitoring and Imaging, Nanomedicine 6 (5) (2011) 879–898.

[20] L. Fewtrell, Silver Water disinfection and toxicity, Centre For Research into Environment and Health, (2014) , pp. 1–53. www.who.int/water_sanitation_-health/dwq/chemicals/Silver_water_disinfection_toxicity_2014v2.pdf.

[21] E.I. Unuabonah, G.U. Adie, L.O. Onah, O.G. Adeyemi, Multistage optimization of the adsorption of Methylene Blue Dye onto defatted *Carica papaya* seeds, Chem. Eng. J. 155 (2009) 567–579.

[22] G.U. Adie, E.I. Unuabonah, A.A. Adeyemo, O.G. Adeyemi, Biosorptive removal of Pb^{2+} and Cd^{2+} onto novel biosorbent: Defatted *Carica Papaya* seeds, Biomass & Bioenergy 35 (7) (2011) 2517–2525.

[23] E.I. Unuabonah, C. Gunter, J. Weber, S. Lubahn, A. Taubert, Hybrid clay: A new highly efficient adsorbent for water treatment, ACS Sustain. Chem. Eng. 1 (8) (2013) 966–973.

[24] E.I. Unuabonah, A. Adedapo, C.O. Nnamdi, A. Adewale, M.O. Omorogie, K. O. Adebowale, et al., Successful scale-up performance of a novel papaya-clay combo adsorbent: up-flow adsorption of a basic dye, Desalin. Water Treat. (2014) 536–551.

[25] E.I. Unuabonah, M.O. Kolawole, F.O. Agunbiade, M.O. Omorogie, D.T. Koko, C.G. Ugwuja, et al., Novel Metal-Doped Bacteriostatic Hybrid Clay

 http://dx.doi.org/10.1016/j.heliyon.2017.e00379

Composites for Point-of-Use Disinfection of Water, J. Environ. Chem. Eng. 5 (2017) 2128–2141.

[26] K.O. Adebowale, E.I. Unuabonah, B.I. Olu-Owolabi, Adsorption of some heavy metal ions on sulfate- and phosphate-modified Kaolin, Appl. Clay Sci. 29 (2005) 145–148.

[27] C. Karunakaran, P. Vinayagamoorthy, Magnetically Recoverable Fe3O4-Implanted Ag-Loaded ZnO Nanoflakes for Bacteria-Inactivation and Photocatalytic Degradation of Organic Pollutants, New. J. Chem. 40 (2016) 1845–1852.

[28] Agilent, http://www.genomics.agilent.com/biocalculators/calcODBacterial.jsp?_requestid=56013, 2016.

[29] J. Glazyrina, E.M. Materne, T. Dreher, D. Storm, S. Junne, T. Adams, et al., High cell density cultivation and recombinant protein production with Escherichia coli in a rocking-motion-type bioreactor, Microb. Cell Fact. 9 (2010) 42.

[30] P. Samprnpiboon, P. Charnkeitkong, X. Feng, Equilibrium Isotherm Models for Adsorption of Zinc (II) Ion from Aqeous Solution on Pulp Waste, WSEAS Transactions on Environment and Development 10 (2014) 2224–3496.

[31] S.J. Gregg, K.S.W. Sing, Adsorption, Surface Area and Porosity, Academic, New York, 1967.

[32] H. Shahbeig, N. Bagheri, A. Ghorbanian, A. Hallajisani, S. Poorkarimi, A new adsorption isotherm model of aqueous solutions on granular activated carbon, World Journal of Modelling and Simulation 9 (4) (2013) 243–254.

[33] I. Langmuir, The constitution and fundamental properties of solids and liquid, J. Am. Chem. Soc. 38 (11) (1916) 2221–2295.

[34] R. Sips, On the Structure of a Catalyst Surface. II, J. Chem. Phys. 18 (8) (1950) 1024–1026.

[35] A. Gunay, E. Arslankaya, I. Tosun, Lead removal from aqueous solution by Natural and pretreated clinoptilolite: Adsorption equilibrium and Kinetics, J. Hazard. Mat. 146 (2007) 362–371.

[36] R. Sips, On the structure of a catalyst surface, J. Chem. Phys. 16 (1948) 490–495.

[37] M. Tămăşan, V. Simon, Thermal and structural characterization of polyvinyl alcohol-kaolinite nanocomposites, Dig. J. Nanomater. Biostruct. 6 (3) (2011) 1311–1316.

 http://dx.doi.org/10.1016/j.heliyon.2017.e00379

[38] J. González, Ruiz MdC: Bleaching of kaolins and clays by chlorination of iron and titanium, Appl. Clay Sci. 33 (3) (2006) 219–229.

[39] B. Nandi, R. Uppaluri, M. Purkait, Preparation and Characteriziation of Low Cost Ceramic Membranes for Micro-Filtration Applications, Appl. Clay Sci. 42 (2008) 102–110.

[40] I. Fatimah, I. Sahroni, H. Putra, M. Nugraha, Ceramic Membrane Based on TiO2-Modified Kaolinite as a Low Cost Material for Water Filtration, Appl. Clay Sci. 118 (2015) 207–211.

[41] E.I. Unuabonah, K.O. Adebowale, B.I. Olu-Owolabi, Kinetic and Thermo-dynamic studies of the adsorption of lead (II) ions onto phosphate-modified Kaolinite clay, J. Hazard. Mater. 144 (2007) 386–395.

[42] R. Narayan, Advances in Bioceramics and Porous Ceramics VIII: Ceramic Engineering and Science Proceedings, Volume 36, John Wiley & Sons, 2015.

[43] R. Fernandez, F. Martirena, K. Scrivener, The Origin of the Pozzolanic Activity of Calcined Clay Minerals: A Comparison Between kaolinite, Illite, and Montmorillonite, Cem. Concr. Res. 41 (2011) 113–122.

[44] S.M. Hayes, S.A. White, T.L. Thompson, R.M. Maier, J. Chorover, Changes in lead and zinc lability during weathering-induced acidification of desert mine tailings: Coupling chemical and micro-scale analyses, Appl. Geochem. 24 (2009) 2234–2245.

[45] P. Kanmani, Rhim J-W. Properties and characterization of bionanocomposite films prepared with various biopolymers and ZnO nanoparticles, Carbohydr. Polym. 106 (2014) 190–199.

[46] V. Dinesh, P. Biji, A. Ashok, S. Dhara, M. Kamruddin, A. Tyagi, et al., Plasmon-mediated, highly enhanced photocatalytic degradation of industrial textile dyes using hybrid ZnO@ Ag core–shell nanorods, RSC Adv. 4 (103) (2014) 58930–58940.

[47] K.S. Warui, Beneficiation of Low grade Titanium Ores from selected sites in Meru, Murang'a and Tharaka Nithi Counties, Kenya, Kenyatta University, Kenya, 2015.

[48] M. Auta, B. Hameed, Chitosan-Clay Composite as Highly Effective and Low-Cost Adsorbent for Batch and Fixed-Bed Adsorption of Methylene Blue, Chem. Eng. J. 237 (2014) 352–361.

[49] A. Spence, B. Kelleher, FT-IR spectroscopic analysis of Kaolinite-Microbial Interactions, Vib. Spectrosc. 61 (2012) 151–155.

 http://dx.doi.org/10.1016/j.heliyon.2017.e00379

[50] M. Silver, Application of Infrared Spectroscopy to Analysis of Chitosan/Clay Nanocomposite, In: T. Theophile (Ed.), Infrared Spectroscopy-Materaial Science, Engineering and Technology, InTech, Shanghai, 2012.

[51] R. Marchessault, F. Ravenelle, X. Zhu, Polysaccharides for Drug Delivery and Pharaceutical Applications. 18 ed., American Chemical Society, Washington, DC, 2006.

[52] Y. Xu, K. Kim, M. Hanna, D. Nag, Chitosan-starch composite film: preparation and characterization, Ind. Crops Prod. 21 (2) (2005) 185–192.

[53] C. Paluszkiewicz, E. Stodolak, M. Hasik, M. Blazewicz, FT-IR Study of Mntmorillonite-Chitosan Nanocomposite Materials, Spectrochim. Acta Part A 79 (2011) 784–788.

[54] G.Y. Li, X.L. Liu, H.M. Zhang, P.K. Wong, T.C. An, H.J. Zhao, Comparative studies of photocatalytic and photoelctrocatalytic inactivation of *E.coli* in presence of halides, Appl. Catal. B: Environ. 140 (2013) 225–232.

[55] C. Yu, J. Iyadayaraj, Spectroscopic Characterization of Microorganisms by Fourier Transform Infrared Microspectroscopy, Biopolymers 77 (2005) 368–377.

[56] T.I. Lotta, I.S. Salonen, J.A. Virtanen, K.K. Eklund, P.K. Kinnunen, Fourier transform infrared study of fully hydrated dimyristoylphosphatidylglycerol: Effects of sodium on the sn-1'and sn-3'headgroup stereoisomers, Biochemistry 27 (21) (1988) 8158–8169.

[57] S. Kumar, A. Panda, R. Singh, Preparation and Characterization of Acids and Alkali Treated Kaolin Clay, Bull. Chem. React. Eng. Cat. 1 (8) (2013) 61–69.

[58] E.K. Marfo, O.L. Oke, O.A. Afolabi, Chemical composition of papaya (*Carica papaya*) seeds, Food Chem. 22 (4) (1986) 259–266.

[59] G. Aravind, D. Bhowmik, S. Duraivel, G. Harish, Traditional and Medicinal Uses of *Carica papaya*, J. Med. Plants Stud. 1 (1) (2013) 7–15.

[60] G. Hatice, M. Parfait, E. Erdogan, R. Sage, Biopolymer Coated Clay Particles for the Adsorption of Tungsten from Water, Desalination 197 (2006) 165–178.

[61] S.S. Tripathy, J.-L. Bersillon, K. Gopal, Removal of fluoride from drinking water by adsorption onto alum-impregnated activated alumina, Sep. Purif. Technol. 50 (2006) 310–317.

[62] J. Rivera-Utrilla, M. Sanchez-Polo, Adsorption of Cr (III) on ozonised activated carbon: Importance of Cπ—cation interactions, Water Res. 37 (14) (2003) 3335–3340.

 http://dx.doi.org/10.1016/j.heliyon.2017.e00379

[63] H. Zhu, R. Jiang, L. Xiao, Y. Chang, Y. Guan, X. Li, et al., Photocatalytic Decolorization and Degradation of Congo Red on Innovative Crosslinked Chitosan/nano-CdS Composite Catalyst Under Visible Light Irradiation, J. Hazard. Mater. 169 (1-3) (2009) 933–940.

[64] V.T.C. Penna, S.A.M. Martins, P.G. Mazzola, Indentification of bacteria in Drinlking and purified water during the monitoring of a typical water purification system, BMC Public Health 2 (2002) 13.

[65] X. Chen, Modeling of Experimental Adsorption Isotherm Data, Information 6 (2015) 14–22.

[66] F. Brouers, O. Sotolongo, F. Marquez, J.P. Pirard, Microporous and heterogeneous surface adsorption isotherms arising from Levy distributions, Physica A 349 (2005) 271–282.

[67] M. Ghorbani, H. Eisazadeh, A. Ghoreyshi, Removal of Zinc Ions from Aqueous Solution Using Polyaniline Nanocomposite Coated on Rice Husk, Iranica Journal of Energy & Environment 3 (2012) 66–71.

[68] Q. Wu, Y. Wang, Z. Wang, Y.T.W. Zhou, Preparation, Characterization of Formic Acid Modified Clinoptilolite and Bacteria Adsorption, Res. J. Appl. Sci. 8 (2) (2013) 143–147.

[69] J. Rivera-Utrilla, I. Bautista-Toledo, M.A. Ferro-Garcia, C. Moreno-Castilla, Activated carbon surface modifications by adsorption of bacteria and their effect on aqueous lead adsorption, J. Chem. Technol. Biotechnol. 76 (2001) 1209–1215.

[70] A.K. Camper, M.W. LeChevallier, S.C. Broadaway, G.A. McFeters, Growth and persistence of pathogens on granular activated carbon filters, Appl. Environ. Microbiol. 50 (1985) 1378–1382.

[71] R.M. Niemi, I. Heiskanen, R. Heine, J. Rapala, Previously uncultured β-Proteobacteria dominate in biologically active granular activated carbon (BAC) filters, Water Res. 43 (2009) 5075–5086.

[72] A. Borkowski, M. Szala, T. Clapa, Adsorption Studies of the Gram-Negative Bacteria onto Nanostructured Silicon Carbide, Appl. Biochem. Biotechnol. 175 (2015) 1448–1459.

[73] H. Liu, Y. Du, X. Wang, L. Sun, Chitosan kills bacteria through cell membrane damage, Int. J. Food Microbiol. 95 (2004) 147–155.

[74] R.G. Saraiva, J.A. Lopes, J. Machado, P. Gameiro, M.J. Feio, Discrimination of single-porin *Escherichia (E.) coli* mutants by ATR and transmission mode FTIR spectroscopy, J. Biophotonics 7 (6) (2014) 392–400.

http://dx.doi.org/10.1016/j.heliyon.2017.e00379

[75] F. Hamadi, H. Latrache, H. Zahir, A. Elghmari, M. Timinouni, M. Ellouali, The relation between Escherichia Coli surface functional groups composition and their physicochemical properties, Braz. J. Microbiol. 39 (2008) 10–15.

[76] K.A. Bhat, P. Rajangam, S. Dharmalingam, Frabrication and Characterization of Polymethylmethacrylate/polysulphone/β-tricalcium phosphate composite for orthopaedic applications, J. Mater. Sci. 47 (2012) 1038–1045.

[77] R.C. Goy, Dd. Britto, O.B. Assis, A review of the antimicrobial activity of chitosan, Polímeros 19 (3) (2009) 241–247.

[78] A. Munoz-Bonilla, M. Fernandez-Garcia, Polymeric materials with antimicrobial activity, Progr. Polym. Sci. 37 (2012) 281–339.

[79] A.M. Carmona-Ribeiro, L.D. de Melo Carrasco, Cationic antimicrobial polymers and their assemblies, Int. J. Mol. Sci. 14 (2013) 9906–9946.

[80] D. Raafat, K. von Bargen, A. Haas, Sahl H-G. Insights into the mode of Action of Chitosan as Antibacterial Compound, Appl. Environ. Microbiol. 74 (2008) 3764–3773.

[81] T. Undabeytia, R. Posada, S. Nir, I. Galindo, L. Laiz, C. Saiz-Jimenez, et al., Removal of waterborne microorganisms by filtration using clay-polymer complexes, J. Hazard. Mat. 279 (2014) 190–196.

[82] M. Baek, M.K. Kim, H.J. Cho, J.A. Lee, J. Yu, H.E. Chung, et al., Factors influencing the cytotoxicity of zinc oxide nanoparticles: particle size and surface charge, J. Phys. Conf. Ser. 304 (2011).

[83] R.C. Goy, S.T.B. Morais, O.B.G. Assis, Evaluation of the antimicrobial activity of chitosan and its quarternized derivative on *E. coli* and *S. aureus* growth, Revista Brasileira de Framacognosia 26 (2016) 122–127.

 http://dx.doi.org/10.1016/j.heliyon.2017.e00379